**Biological Sciences**

# A bacterial effector protein prevents MAPK-mediated phosphorylation of SGT1 to suppress plant immunity

Gang Yu[1], Liu Xian[1,2], Hao Xue[1,2], Wenjia Yu[1,2], Jose Rufian[1], Yuying Sang[1], Rafael Morcillo[1], Yaru Wang[1,2], and Alberto P. Macho[1,*].

[1]Shanghai Center for Plant Stress Biology, CAS Center for Excellence in Molecular Plant Sciences; Shanghai Institutes of Biological Sciences, Chinese Academy of Sciences, Shanghai 201602, China.

[2]University of Chinese Academy of Sciences, Beijing, China.

* Corresponding author: Alberto P. Macho, alberto.macho@sibs.ac.cn

**Keywords: NLR; SGT1; MAPK; ETI; effector; immunity; phosphorylation; virulence; Ralstonia.**

**Abstract**

Nucleotide-binding domain and leucine-rich repeat-containing (NLR) proteins function as sensors that perceive pathogen molecules and activate immunity. In plants, the accumulation and activation of NLRs is regulated by SUPPRESSOR OF G2 ALLELE OF *skp1* (SGT1). In this work, we found that the plant pathogen *Ralstonia solanacearum* secretes an effector protein, named RipAC, inside plant cells, and it associates with SGT1 to suppress NLR-mediated SGT1-dependent immune responses. RipAC does not affect the accumulation of SGT1, NLRs, or their interaction. However, RipAC inhibits the interaction between SGT1 and MAP kinases, and the phosphorylation of a MAPK target motif in the C-terminal domain of SGT1, which is required for the interaction with NLRs. Such phosphorylation releases the interaction between SGT1 and the NLR RPS2, and contributes to the activation of RPS2-mediated responses. Our results shed light onto the mechanism of activation of NLR-mediated immunity, and suggest a positive feedback loop between MAPK activation and SGT1-dependent NLR activation.

**Significance Statement**

The activation of immune receptors that perceive pathogen molecules and initiate immune signaling is tightly regulated. In plants and animals, SGT1 is a major regulator of the accumulation and activation of such receptors, although the mechanisms of this regulation are not well understood. In this work, we found that the plant pathogenic bacteria *Ralstonia solanacearum*, causal agent of the bacterial wilt disease, secretes an effector protein inside plant cells that suppresses the phosphorylation-dependent activation of SGT1, which in turn inhibits the activation of SGT1-dependent immune receptors. These findings provide new insights into a general mechanism of regulation of immunity, and uncover a new virulence strategy employed by a bacterial pathogen to contribute to disease development.

## Introduction

The activation and suppression of plant immunity are key events that determine the outcome of the interaction between plants and bacterial pathogens. When in close proximity to plant cells, conserved bacterial molecules (termed PAMPs, for pathogen-associated molecular patterns) may be perceived by receptors at the surface of plant cells, eliciting the activation of the plant immune system. This leads to the establishment of PAMP-triggered immunity (PTI; (1)), which restricts bacterial growth and prevents the development of disease. Most bacterial pathogens have acquired the ability to deliver proteins inside plant cells via a type-III secretion system (T3SS); such proteins are thus called type-III effectors (T3Es) (2). Numerous T3Es from adapted bacterial plant pathogens have been reported to suppress PTI (3). This, in addition to other T3E activities (4), enables bacterial pathogens to proliferate and cause disease. Resistant plants have evolved mechanisms to detect such bacterial manipulation through the development of intracellular receptors defined by the presence of nucleotide-binding sites (NBS) and leucine-rich repeat domains (LRRs), thus termed NLRs (5). The detection of T3E activities through NLRs leads to the activation of immune responses, which effectively prevent pathogen proliferation (6). The outcome of these responses is named effector-triggered immunity (ETI), and, in certain cases, may cause a hypersensitive response (HR) that involves the collapse of plant cells. In an evolutionary response to this phenomenon, T3E activities have evolved to suppress ETI (7), which in turn exposes bacterial pathogens to further events of effector recognition. For these reasons, the interaction between plants and

microbial pathogens is often considered an evolutionary ‘arms race’, where the specific combination of virulence activities and immune receptors in a certain pathogen-plant pair ultimately defines the outcome of the interaction (7). Although the suppression of PTI by T3Es has been widely documented (3), reports about T3Es that suppress ETI, and their biochemical characterization, remain scarce.

Interestingly, PTI and ETI signaling often involve shared regulators (8), such as mitogen-activated protein kinases (MAPK). The activation of MAPKs is one of the earliest signaling events upon perception of both PAMPs and effectors (9), and is essential for the activation of immune responses. Although sustained MAPK activation has been reported to be critical for the robust development of ETI (10), the signaling events and phosphorylation substrates that link early MAPK activation upon pathogen recognition and downstream MAPK activation as a consequence of NLR activation remain unknown.

The study of microbial effectors has become a very prolific approach to discover and characterize components of the plant immune system and other cellular functions that play important roles in plant-microbe interactions (11). In this regard, T3E repertoires constitute a powerful tool for researchers to understand plant-bacteria interactions. The *Ralstonia solanacearum* species complex (RSSC) groups numerous bacterial strains able to cause disease in more than 250 plant species, including important crops, such as tomato, potato, and pepper, among others (12, 13). *R. solanacearum*

invades the roots of host plants, reaching the vascular system and colonizing xylem vessels in the whole plant, eventually causing their blockage and subsequent plant wilting (14, 15). It has been speculated that the versatility and wide host range of *R. solanacearum* is associated to its relatively large T3E repertoire in comparison with other bacterial plant pathogens; the reference GMI1000 strain serves as an example, being able to secrete more than 70 T3Es (16). Among these T3Es, RipAC (also called PopC; (16, 17)) is conserved in most *R. solanacearum* sequenced to date, and is therefore considered a core T3E in the RSSC (Figures S1A and S1B) (16). Domain prediction for the RipAC amino acid sequence reveals the presence of an LRR C-terminal domain and no other predicted enzymatic domain (Figure S1C). Interestingly, it has been shown that RipAC from different *R. solanacearum* strains is promptly expressed upon bacterial inoculation in different host plants (18, 19) suggesting a role in the establishment of the interaction at early stages of the infection process.

## Results

### RipAC contributes to *Ralstonia solanacearum* infection

It is well established that T3Es collectively play an essential role in the development of disease caused by most bacterial plant pathogens, including *R. solanacearum* (20). To study the contribution of RipAC to *R. solanacearum* infection, we generated a *ΔripAC* mutant strain using the reference phylotype I GMI1000 strain as background (Figure S1D), and confirmed that the growth of this strain in rich laboratory medium is indistinguishable from the wild-type (WT) strain (Figures S1D-1G). We then performed soil-drenching inoculation of Arabidopsis Col-0 WT plants with both WT and *ΔripAC* strains, and monitored the development of wilting symptoms associated to disease. Compared with plants inoculated with WT GMI1000, plants inoculated with the *ΔripAC* mutant displayed attenuated disease symptoms (Figure 1A). This attenuation was complemented by the expression of *ripAC*, driven by its native promoter, in the *ΔripAC* mutant background (Figures 1A and S1E-1G), confirming that virulence attenuation was indeed caused by the lack of the *ripAC* gene. Given the intrinsic complexity and biological variability of the soil-drenching inoculation assay, we did not detect a significant attenuation every time we performed this experiment (Figure S2A), suggesting that the attenuation caused by the absence of RipAC is near the limit of detection of this assay. Tomato is a natural host for several *R. solanacearum* strains (21). As observed in Arabidopsis, tomato plants inoculated with the *ΔripAC* strain showed delayed and/or reduced symptom development in most

experiments (Figures 1B and S2B). This attenuation was complemented by the expression of *ripAC* in the mutant background (Figure 1B).

In order to increase the accuracy of our virulence assays and to determine whether the reduced disease symptoms correlate with reduced bacterial multiplication inside host plants, we set up an assay to quantify bacterial numbers in the xylem sap of tomato plants upon injection of the bacterial inoculum in the stem. Compared to plants inoculated with WT GMI1000 or the complementation strain, plants inoculated with the *ΔripAC* strain showed reduced bacterial numbers (Figure 1C). Altogether, these results suggest that, despite the large effector repertoire of *R. solanacearum* GMI1000, RipAC plays a significant role during the infection process in different host plants.

To complement our genetic analysis of the importance of RipAC in promoting susceptibility to *R. solanacearum*, we generated stable Arabidopsis transgenic lines expressing RipAC from a 35S constitutive promoter (Figures S3A and S3B). Independent transgenic lines expressing RipAC showed enhanced disease symptoms upon soil-drenching inoculation with *R. solanacearum* (Figures 1D and S3C), indicating that RipAC promotes susceptibility to *R. solanacearum* from within plant cells.

**RipAC interacts with SGT1 from different plant species**

Upon transient expression in *Nicotiana benthamiana*, RipAC fused to a C-terminal GFP tag shows a sharp signal at the cell periphery of leaf epidermal cells (Figure S4A). Fractionation of protein extracts from *N. benthamiana* expressing RipAC, showed abundant RipAC in both microsomal and cytosolic fractions (Figure S4B). To identify plant proteins that physically associate with RipAC in plant cells, we performed immunoprecipitation (IP) of RipAC-GFP using GFP-trap agarose beads, and analyzed its interacting proteins using liquid chromatography coupled to tandem mass-spectrometry (LC-MS/MS). Together with RipAC-GFP immunoprecipitates, we identified peptides of NbSGT1 (Figure S5A), homolog of the Arabidopsis SUPPRESSOR OF G2 ALLELE OF *skp1* (SGT1), a protein required for the induction of disease resistance mediated by most NLRs (22, 23). The localization of both isoforms of SGT1 in Arabidopsis (AtSGT1a and AtSGT1b) has been reported to be nucleocytoplasmic (24). When we expressed SGT1 (NbSGT1, AtSGT1a, or AtSGT1b) fused to a C-terminal RFP tag, we also detected an apparently cytoplasmic localization, with occasional nuclear localization, although we also detected co-localization with the plasma membrane marker CBL-GFP ((25); Figures S5B and S5C). Interestingly, we detected co-localization between RipAC-GFP and NbSGT1-RFP, AtSGT1a-RFP, or AtSGT1b-RFP (Figure S5D). These results also suggest that RipAC does not affect SGT1 subcellular localization. To confirm the physical interaction between RipAC and SGT1 from different plant species, we co-expressed RipAC-GFP with either NbSGT1, AtSGT1a, AtSGT1b or the tomato ortholog of SGT1b (SlSGT1b). Targeted IP of RipAC-GFP showed CoIP of all

different SGT1 orthologs (Figure 2A). Similarly, split-luciferase complementation (Split-LUC) assays showed luciferase signal upon expression of RipAC with AtSGT1a, AtSGT1b or NbSGT1 fused to different luciferase halves (Figure 2B). We also performed similar split-YFP assays, showing reconstitution of YFP signal at the cell periphery upon expression of RipAC and AtSGT1a, AtSGT1b or NbSGT1 tagged with one of the portions of a split-YFP molecule (Figure S5E), indicating a direct interaction of these proteins at the cell periphery. Altogether, these results indicate that RipAC physically associates with SGT1 from different species inside plant cells.

SGT1 is conserved in eukaryotes, and has three defined domains: an N-terminal tetratricopeptide repeat (TPR) domain, a CHORD-SGT1 (CS) domain, and a C-terminal SGT1-specific (SGS) domain (26). In order to determine which NbSGT1 domain is required for RipAC interaction, we expressed different combinations of these domains (Figure S5F) bound to a FLAG tag, and tested their interaction with immunoprecipitated RipAC-GFP. Although we were unable to express the SGS domain alone, we detected interaction between RipAC and a truncated SGT1 protein containing the CS+SGS domain (Figure S5F). The CS domain alone did not interact with RipAC, suggesting that RipAC associates with the SGS domain, although it cannot be ruled out that RipAC requires both CS+SGS domains to associate with SGT1. Interestingly, the SGS domain is required for all the known SGT1b functions in immunity (24, 26).

198 SGT1 physically associates with several NLRs (27-29); here we found that AtSGT1b
199 also interacts with the NLR RPS2 (30) (Figure S5G). To determine whether RipAC
200 interferes with the interaction between SGT1 and NLRs, we performed Split-LUC
201 assays between AtSGT1b and RPS2 in the presence of RipAC. Interestingly, RipAC
202 did not affect RPS2 accumulation or the interaction between AtSGT1b and RPS2
203 (Figures S5G and S5H).
204
205 **RipAC inhibits SGT1-mediated immune responses in *N. benthamiana* and**
206 **Arabidopsis**
207 To determine whether RipAC has the potential to suppress SGT1-mediated immune
208 responses, we first performed transient expression of RipAC-GFP in *N. benthamiana*,
209 and monitored the induction of cell death associated to the hypersensitive response
210 (HR) developed as part of an ETI response, such as that triggered by overexpression
211 of the NLR-encoding gene *RPS2* (31), the expression of the oomycete effector Avr3a
212 together with the cognate NLR R3a (32), and that triggered by inoculation with *P.*
213 *syringae* pv. *tomato* DC3000 (*Pto* DC3000) (33). RipAC suppressed the HR triggered
214 by RPS2 and Avr3a/R3a, while it attenuated and delayed HR development in
215 response to *Pto* DC3000 (Figure 2C), showing the potential of RipAC to suppress ETI.
216 We have recently reported that the *R. solanacearum* T3E RipE1 triggers
217 SGT1-dependent immunity in *N. benthamiana* (34). RipAC was also able to suppress
218 RipE1-induced HR (Figure 2C). Interestingly, RipAC was not able to suppress the cell
219 death triggered by other elicitors, such as Bax (35) and the oomycete elicitor INF1 (36)

220 (Figure 2D), suggesting that RipAC is not a general suppressor of cell death. Ion
221 leakage measurements validated that RipAC suppresses SGT1-dependent
222 ETI-associated cell death (e.g. triggered by RPS2 or RipE1), but had a minor impact
223 on BAX-triggered cell death (Figure S6A and S6B).
224
225 The activation of NLRs is known to trigger the activation of mitogen-activated protein
226 kinases (MAPKs; (10, 37)). Consistently, transient overexpression of RPS2 in *N.*
227 *benthamiana* leads to an activation of MAPKs that precedes the onset of ion leakage
228 and macroscopic cell death (Figures S6A-S6D). In our transient expression assays,
229 RipAC significantly suppressed the activation of MAPKs triggered by overexpression
230 of RPS2, Avr3a/R3a, or by the expression of RipE1 (Figures 2E-2G and 2I),
231 supporting the notion that RipAC suppresses early steps in ETI activation rather than
232 downstream responses that lead to cell death. In agreement with this, RipAC also
233 abolished the macroscopic cell death and MAPK activation triggered by the
234 overexpression of a constitutively active form of the Arabidopsis MAPK Kinase 7
235 (AtMKK7DD) in *N. benthamiana* (Figures 2C and 2H-2I), which requires SGT1
236 function (38).These results indicate that RipAC is able to suppress ETI-associated
237 SGT1-dependent responses from different origins in *N. benthamiana*.
238
239 To determine whether RipAC inhibits the final outcome of ETI (i.e. restriction of
240 bacterial proliferation), we inoculated RipAC-expressing Arabidopsis transgenic lines
241 (Figures S3A and S3B) with *Pto* DC3000 expressing different T3Es that activate

NLR-dependent immunity, namely AvrRpm1 (39), AvrRpt2 (30), or AvrRps4 (40). Such strains, compared to *Pto* DC3000 expressing an empty vector (EV) (Figure 2J), show deficient replication in Arabidopsis, due to immune responses triggered by these T3Es (Figures 2K-2M). However, transgenic lines expressing RipAC showed enhanced susceptibility to these strains (Figures 2K-2M), indicating that RipAC is able to effectively suppress NLR-mediated immunity in Arabidopsis.

**MAPK-mediated phosphorylation is important for SGT1 function in the activation of ETI**

Since post-translational modifications (PTMs) have been shown to impact SGT1 function (41-43), we sought to determine whether RipAC causes any alteration of SGT1 PTMs in plant cells. To this end, we co-expressed NbSGT1 fused to a FLAG tag together with RipAC (or a GFP control) in *N. benthamiana* leaves, and then performed IP using an anti-FLAG resin followed by LC-MS/MS. Among the IPed SGT1 peptides, we detected two peptides, located in the SGS domain, containing phosphorylated serine residues (S282 and S358) (Figure S7). Interestingly, a phosphorylable residue is conserved in these positions among plants from different species (Figures S8A), and S358 is embedded in a canonical MAPK-mediated phosphorylation motif conserved across the plant kingdom (Figure S8B). Interestingly, AtSGT1b has been shown to interact with MAPK4 (44), and SGT1 from tobacco (NtSGT1) S358, equivalent to T346 in AtSGT1b, has been shown to be phosphorylated by NtSIPK (41). By performing targeted CoIP, we found that both

264 AtSGT1a and AtSGT1b associate with AtMAPK4 and AtMAPK6, but not with
265 AtMAPK3, which showed very low accumulation in this assay (Figure 3A). The
266 association of both AtSGT1a and AtSGT1b with AtMAPK3 and AtMAPK4, but not with
267 AtMAPK6, was also shown by Split-LUC (Figure S9). To determine whether
268 MAPK-mediated SGT1 phosphorylation is enhanced upon activation of ETI, we raised
269 an antibody against the potential MAPK phosphorylated peptide, conserved in both
270 AtSGT1a and AtSGT1b, containing phosphorylated T346 (ESpTPPDGME), which
271 specifically detected the phosphorylated peptide *in vitro* and *in planta* (Figures S10A
272 and S10B). Inoculation of Arabidopsis plants with *Pto* expressing AvrRpt2 or
273 AvrRps4, but not with *Pto* DC3000 or *Pto* TTSS$^{-}$, led to a sustained activation of
274 MAPKs and to enhanced phosphorylation of T346 (Figure S10C). Similarly,
275 dexamethasone-induced expression of AvrRpt2 in Arabidopsis transgenic lines led to
276 sustained MAPK activation and enhanced SGT1 phosphorylation (Figures 3B and
277 3C). These data indicate that an enhancement of T346 phosphorylation occurs
278 concomitantly to the activation of ETI.
279
280 To determine the relevance of the phosphorylation of SGT1 S271/T346 for the
281 activation of ETI, we generated single and double point mutants in these residues in
282 AtSGT1b, substituting them for alanine residues (to abolish phosphorylation) or for
283 aspartate residues (to mimic the negative charge associated to constitutive
284 phosphorylation). Due to the difficulties in performing genetic analysis of SGT1, we
285 used a transient approach in *N. benthamiana*, co-expressing the AtSGT1b variants

together with RPS2. Alanine mutations (S271A/T346A: AtSGT1b AA) did not have a detectable impact on the RPS2-mediated cell death (Figure 3D), likely due to the presence of endogenous NbSGT1. However, tissues expressing both the T346D mutant (2D) or the double S271D/T346D (DD) mutant, but not the single S271D mutant, showed an enhancement of cell death triggered by RPS2 expression, monitored as ion leakage (Figure 3D), which correlated with the appearance of tissue necrosis (Figures 3E and 3F). Similarly, co-expression with the 2D mutant enhanced cell death triggered by RipE1 and Avr3a/R3a (Figure S10D and S10E), but not BAX (Figure S10F). This suggests that T346 phosphorylation contributes to the robust activation of SGT1-dependent ETI responses, including that triggered by the *R. solanacearum* T3E RipE1.

Given the importance of protein-protein interactions in the SGT1 complex, we hypothesized that phosphorylation in S271/T346 may be important to regulate the interaction of SGT1 with NLRs. Interestingly, the T346A mutation did not affect the interaction between AtSGT1b and RPS2 (Figure 3G and S10G-H); however, surprisingly, the T346D mutation inhibited this interaction (Figure 3G and S10G-H). This, together with the observation that the T346D mutation causes an enhancement of RPS2-triggered responses, suggests a scenario where phosphorylation contributes to the release of RPS2 from the SGT1 complex to activate immune responses.

**RipAC interferes with the MAPK-SGT1 interaction to suppress SGT1 phosphorylation**

During our analysis of SGT1 phosphorylation, we observed an apparent reduction in the number of SGT1 phosphorylated peptides in the presence of RipAC (Figure S7A). Since this assay does not allow a comparative quantitative assessment of SGT1 phosphorylation, we took advantage of the sensitivity of our anti-pSGT1 antibody to determine the impact of RipAC on the phosphorylation of AtSGT1 T346. Interestingly, Arabidopsis transgenic lines expressing RipAC showed reduced phosphorylation of T346 in endogenous SGT1 in basal growth conditions (Figures 4A and 4B). Such reduction of T346 phosphorylation was also observed when Arabidopsis protoplasts were transfected with RipAC in the presence of AvrRpt2 (Figures S11A and S11B). We then generated Arabidopsis transgenic lines expressing RipAC and dexamethasone-inducible AvrRpt2 by crossing. RipAC completely abolished MAPK activation and T346 phosphorylation induced by the expression of AvrRpt2 (Figure 4C and 4D). Altogether, these data indicate that RipAC suppresses the phosphorylation of AtSGT1 T346, and provides an additional link between MAPK activation and SGT1 phosphorylation. We considered the possibility that RipAC suppresses SGT1 phosphorylation by interfering with the MAPK-SGT1 interaction. This interference was indeed confirmed by Split-LUC and CoIP assays, which showed that RipAC inhibits the interaction of SGT1 with all AtMAPK3, AtMAPK4 and AtMAPK6 (Figures 4E-4G, S11C-S11E), suggesting that this is the mechanism underlying RipAC suppression of SGT1-dependent ETI responses (Figure S12).

## Discussion

Plant invasion by bacterial pathogens leads to the recognition of bacterial elicitors, either PAMPs or effectors, which, in turn, promotes the production and activation of additional immune receptors. Such feedback loop contributes to the robustness of the plant immune system. To achieve a successful infection and establish a compatible interaction, bacteria should evolve to suppress the activation of the immune responses triggered by the recognition of their PAMPs or effectors. Despite the importance of T3Es for the bacterial infection process, single effector knockout mutants often lack virulence phenotypes due to functional redundancy among effectors. This may be particularly important in strains belonging to the *R. solanacearum* species complex, where single strains may secrete more than 70 T3Es (16). Although such large number of effectors contribute to the infection process, this also poses a risk for *R. solanacearum*, since each effector could potentially be recognized by intracellular NLRs, resulting in ETI. To maintain pathogenicity, bacterial pathogens need to adapt to new recognition events by losing these recognized effectors or evolving additional effectors that suppress ETI. This pathoadaptation becomes evident in the case of RipE1: a *R. solanacearum* GMI1000 derivative strain carrying mutations in *popP1* and *avrA* is pathogenic in *N. benthamiana* (45), despite secreting RipE1, which activates ETI in this plant species (34). This suggests that *R. solanacearum* has evolved T3Es that suppress immunity triggered by RipE1 (and potentially other T3Es). We have shown that RipE1-triggered immunity requires SGT1

351 (34). In this work, we show that SGT1 phosphorylation contributes to RipE1-triggered
352 cell death, which further supports the relevance of the SGT1 immunity node and
353 SGT1 phosphorylation in the context of *R. solanacearum* infection. Accordingly,
354 RipAC inhibits RipE1-triggered cell death. Altogether, this suggests that RipAC may
355 contribute to *R. solanacearum* infection process by inhibiting SGT1-dependent
356 immunity triggered by RipE1 and potentially other T3Es. Before, a *ΔripAC* mutant
357 strain was reported to show reduced fitness, compared to GMI1000, in eggplant
358 leaves (46). Here we show that an equivalent mutant has impaired virulence in
359 Arabidopsis and tomato, and such attenuation is complemented by the expression of
360 the effector, indicating that RipAC plays a significant role in the *R. solanacearum*
361 infection process. It is noteworthy that, despite the ETI-suppressing activity of RipAC,
362 the *ΔripAC* mutant strain showed virulence attenuation instead of eliciting ETI,
363 reflecting a certain degree of redundancy with other ETI-suppressing T3Es, such as
364 RipAY (34, 47).
365
366 In this work, we found that RipAC interacts with SGT1, a major regulator of the activity
367 of NLRs in the activation of ETI (26). SGT1 has been shown to regulate NLR
368 homeostasis, either by contributing to protein stability or by mediating their
369 degradation (48, 49). RipAC was able to interact with a truncated SGT1 containing
370 only the CS+SGS domains, but not with the CS domain alone, suggesting that RipAC
371 interacts with the SGS domain, or that it requires both CS and SGS domains for
372 interaction. The SGS domain is essential for SGT1 immune functions and mediates

SGT1 interaction with the LRRs of NLRs and the co-chaperone HSC70 (24), although its biochemical function remains unclear.

We found that RipAC prevents the interaction between MAPKs and SGT1 in plant cells, leading to a reduced phosphorylation of SGT1 in the SGS domain, suggesting that MAPKs also interact with this domain. MAPKs have been shown to phosphorylate SGT1 from tobacco and maize in *N. benthamiana* (41, 43), contributing to the hypothesis that MAPK-mediated phosphorylation of SGT1 may be important for its function. This notion is also supported by our data, showing that mutations that mimic phosphorylation in the observed SGT1 phosphosites lead to an enhanced activity of the NLR RPS2 (Figure S12). Interestingly, the enhanced RPS2 activity caused by the T346D phospho-mimic mutation correlated with an enhanced dissociation between SGT1 (T346D) and RPS2, suggesting that MAPK-mediated phosphorylation of SGT1 may contribute to NLR activation through the modulation of SGT1 interactions with NLRs (Figure S12). Considering that NLR activation leads to enhanced MAPK activation, this regulatory mechanism would represent a positive feedback loop between the activation of NLRs and MAPKs, mediated by the phosphorylation of SGT1 (Figure S12). Intriguingly, although RipAC suppresses SGT1-dependent immune responses, it does not seem to affect the accumulation of SGT1 or NLRs (in our case, RPS2), which resembles the phenotype observed upon overexpression of the SGS-interacting protein HSC70 (24). Moreover, a mutant including a premature stop codon at P347 in AtSGT1b (disrupting the MAPK phosphorylation motif that

395 includes T346) does not affect SGT1 accumulation, but abolishes the
396 immune-associated functions of SGT1 (50), highlighting the importance of the MAPK
397 phosphorylation motif for SGT1 function. Altogether, our data suggest that, by
398 associating with the SGS domain, RipAC compromises SGT1 interaction with MAPKs
399 and the subsequent phosphorylation of specific sites in the SGS domain,
400 compromising the activation of immunity without altering the accumulation of
401 associated proteins (Figure S12).
402
403 Although the contribution of SGT1 to the establishment of ETI is well known, genetic
404 analysis of its contribution to disease resistance is challenging, due to the deleterious
405 effects caused by the abolishment of SGT1 expression (26). However, Arabidopsis
406 transgenic plants expressing RipAC become more susceptible to *R. solanacearum*
407 infection, suggesting the importance of SGT1 function for resistance against *R.*
408 *solanacearum*, although we should consider that other potential targets of RipAC may
409 also account for the enhanced susceptibility of RipAC-expressing transgenic plants.
410
411 The T3E AvrBsT from *Xanthomonas campestris* also interacts with SGT1 from pepper,
412 and interferes with its phosphorylation by the PIK1 kinase in two serine residues (in
413 the CS domain and variable region) different from the ones identified in our study (42).
414 However, in that case, AvrBsT triggers SGT1-mediated immunity, and the identified
415 SGT1 phosphorylation sites are required for the activation of AvrBsT-triggered HR
416 (42). Similarly, a secreted effector from the fungal pathogen *Ustilago maydis* also

interferes with the MAPK-mediated phosphorylation of SGT1 from maize in a monocot-specific phosphorylation site between TPR and CS domains, contributing to the development of disease-associated tumors (43). This demonstrates that pathogens from different kingdoms and with different lifestyles have evolved to target different functions of SGT1 as a key regulator of disease resistance. However, some of these effectors are indeed perceived by the plant immune system, potentially as a consequence of the 'guarding' of SGT1 as an important regulator of plant immunity. On the contrary, RipAC seems to manipulate SGT1 for virulence purposes without being detected by the plant immune system, suggesting that these host plants have not yet evolved a perception system for this targeting. Together with other reports, our discovery of the molecular mechanisms underlying the RipAC-mediated suppression of SGT1 function may contribute to the engineering of functional SGT1 complexes that abolish bacterial manipulation or respond to it by activating immunity.

## Materials and methods

All the experimental procedures are detailed in the supporting Materials and Methods section. The biological and chemical resources used in this study are summarized in the Table S1.

## Acknowledgements

We thank Nemo Peeters and Anne-Claire Cazale for sharing unpublished biological materials, Yasuhiro Kadota and Ken Shirasu for helpful discussions and sharing biological materials, Suomeng Dong, Jian-Min Zhou, Gitta Coaker, and Laurent

Deslandes for sharing biological materials, Rosa Lozano-Duran for critical reading of this manuscript, and Xinyu Jian for technical and administrative assistance during this work. We thank the PSC Cell Biology and Proteomics core facilities for assistance with confocal microscopy and LC-MS/MS analysis, respectively. This work was supported by the Strategic Priority Research Program of the Chinese Academy of Sciences (grant XDB27040204), the National Natural Science Foundation of China (NSFC; grant 31571973), the Chinese 1000 Talents Program, and the Shanghai Center for Plant Stress Biology (Chinese Academy of Sciences). Gang Yu was partially supported by the China Postdoctoral Science Foundation (grant 2016M600339). The authors have no conflict of interest to declare.

452 **Figure legends**

453 **Figure 1. RipAC contributes to *Ralstonia solanacearum* virulence in**
454 **Arabidopsis and tomato.** (A, B) Soil-drenching inoculation assays in Arabidopsis (A)
455 and tomato (B) were performed with GMI1000 WT, Δ*ripAC* mutant, and RipAC
456 complementation (*ripAC*$^+$) strains. n=15 plants per genotype (for Arabidopsis) or n=12
457 plants per genotype (for tomato). The results are represented as disease progression,
458 showing the average wilting symptoms in a scale from 0 to 4 (mean ± SEM). (C)
459 Growth of *R. solanacearum* GMI1000 WT, Δ*ripAC* mutant, and RipAC
460 complementation (*ripAC*$^+$) strains in tomato plants. 5 µL of bacterial inoculum ($10^6$ cfu
461 $mL^{-1}$) were injected into the stem of 4-week-old tomato plants and xylem sap was
462 taken from each infected plants for bacterial titer calculation 3 days post-inoculation
463 (dpi) (mean ± SEM, n=6, ** $p<0.01$, *t*-test). (D) Soil-drenching inoculation assays in
464 Col-0 WT and RipAC-expressing Arabidopsis lines (AC #3, AC #31, two independent
465 lines) with GMI1000 WT strain. Results are represented as in A and B.
466 See also Figures S1-S3.
467

468 **Figure 2. RipAC inhibits SGT1-dependent immune responses.**
469 (A) CoIP to determine interactions between RipAC and SGT1s. The signal in the
470 interaction between RipAC and AtSGT1a was weak and is shown with longer
471 exposure. (B) Split-LUC assay to determine direct interaction between RipAC and
472 SGT1 in plant cells. (C) RipAC suppresses RPS2-, Avr3a/R3a-, *Pto* DC3000-, RipE1-,
473 or AtMKK7DD-associated cell death. (D) RipAC does not suppress BAX- or

INF1-induced cell death. Photographs were taken 5 days after the expression of the cell death inducer. The numbers beside the photographs indicate the ratios of infiltrations showing the presented result among the total number of infiltrations. (E-F) RipAC suppresses MAPK activation triggered by the overexpression of RPS2 (E), Avr3a/R3a (F), RipE1 (G) or AtMKK7DD (H). Plant tissues were taken one day after expression of the cell death inducer. (I) Quantification of relative pMAPK in (E-F). The quantification of the pMAPK band in RipAC expression lanes is represented relative to the intensity in the control expressing GFP in each assay (mean ± SEM of 3 or 4 independent biological replicates). (J-M) RipAC suppresses effector-triggered immunity in Arabidopsis. Leaves of WT (WT) and RipAC-transgenic lines (AC #3 and AC #31) were hand-infiltrated with *Pto* empty vector (EV, J), *Pto* AvrRpm1 (K), *Pto* AvrRpt2 (L), or *Pto* AvrRps4 (M). Samples were taken 3dpi (mean ± SEM, n=6, ** $p<0.01$, *t*-test). These experiments were repeated at least 3 times with similar results. See also Figures S4-S6.

**Figure 3. MAPK-mediated phosphorylation is important for SGT1 function in the activation of ETI.**

(A) AtSGT1a and AtSGT1b associate with MAPK4 and MAPK6 in plant cells. CoIPs were performed as in Fig. 2A. (B) MAPK activation triggered by AvrRpt2 expression correlates with increased AtSGT1 phosphorylation at T346. Twelve-day-old Dex:AvrRpt2/Col-0 crossing F1 plants were treated with 30 mM Dex, and samples were taken at the indicated time points. A custom antibody was used to detect the

phosphorylated peptide containing AtSGT1 T346. The induction of AvrRpt2 was determined by RT-PCR. (C) Quantification of pSGT1b signal relative to coomassie blue staining control in (B) (mean ± SEM of 6 independent biological repeats, p-values are shown, *t*-test). (D) A phospho-mimic mutation in AtSGT1b T346 (T346D) promotes cell death triggered by RPS2 overexpression. Agrobacterium expressing AtSGT1b variants or the GUS-FLAG control (OD600=0.5) were infiltrated into *N. benthamiana* leaves 1 day before infiltration with Agrobacterium expressing RPS2 (OD600=0.15). Leaf discs were taken 21 hpi for conductivity measurements at the indicated time points. The time points in the x-axis are indicated as hpi with Agrobacterium expressing RPS2 (mean ± SEM, n=4, ** $p<0.01$, *t*-test, 3 replicates). (E, F) Observation of RPS2-triggered cell death by visible light (E) and UV light (F). The Agrobacterium combinations were infiltrated as described in (D), and the cell death phenotype was recorded 4 dpi with Agrobacterium expressing RPS2. (G) A phospho-mimic mutation in AtSGT1b T346 (T346D) disrupts RPS2-SGT1b association. Quantitation of the luciferase signal was performed with microplate luminescence reader (mean ± SEM, n=8, ** $p<0.01$, *t*-test, 3 replicates). The nomenclature of the AtSGT1b mutants used is: 1A=S271A, 1D=S271D, 2A=T346A, 2D=T346D, AA=S271AT346A, DD=S271DT346D. The experiments were performed at least 3 times with similar results.

See also Figures S7-S10.

**Figure 4. RipAC interferes with MAPK-SGT1 interaction to suppress SGT1 phosphorylation.**

(A) RipAC reduces SGT1 phosphorylation in Arabidopsis. SGT1 phosphorylation was determined in twelve-day-old Col-0 WT and RipAC transgenic lines (AC #3 and AC #31) by western blot. Custom antibodies were used to detect the accumulation of SGT1 and the presence of a phosphorylated peptide containing AtSGT1 T346. (B) Quantification of SGT1 and pSGT1b signal normalized to actin and relative to Col-0 WT samples in (A) (mean ± SEM, n=9, p-values are shown, *t*-test). (C) RipAC suppresses ETI-triggered SGT1 phosphorylation in Arabidopsis. ETI triggered MAPK activation and SGT1 phosphorylation were determined in twelve-day-old Dex::AvrRpt2/RipAC crossing F1 plants by western blot. Custom antibodies were used to detect the accumulation of SGT1 and the presence of a phosphorylated peptide containing AtSGT1 T346. The induction of AvrRpt2 was determined by RT-PCR. The Dex:AvrRpt2/Col-0 panel shows an independent replicate of the experiment shown in Figure 3B, included here as control. (D) Quantification of pSGT1b signal relative to coomassie blue staining control in the Dex:AvrRpt2/AC#3 panel shown in (C) (mean ± SEM of 6 independent biological replicates, p-values are shown, *t*-test), for comparison with the quantitation shown in Figure 3C. (E, F) Competitive Split-LUC assays showing that RipAC interferes with the interaction between MAPK3 (E) / MAPK4 (F) and AtSGT1b. In quantitative assays, the graphs show the mean value ± SEM (n=8, ** $p<0.01$, *t*-test). (G) Competitive CoIP showing that RipAC interferes with the interaction between MAPK6 and AtSGT1b. Anti-FLAG

beads were used to IP MAPK6. In all the competitive interaction assays, in addition to the interaction pair, RipAC or CBL-GFP (as negative control) were expressed to determine interference. In all the blots, asterisks indicate non-specific bands. These experiments were repeated at least 3 times with similar results.

See also Figures S11.

**References**


1. Boller T & Felix G (2009) A renaissance of elicitors: perception of microbe-associated molecular patterns and danger signals by pattern-recognition receptors. *Annual Review of Plant Biology* 60(1):379-406.
2. Galán JE, Lara-Tejero M, Marlovits TC, & Wagner S (2014) Bacterial type III secretion systems: specialized nanomachines for protein delivery into target cells. *Annual Review of Microbiology* 68(1):415-438.
3. Macho AP & Zipfel C (2015) Targeting of plant pattern recognition receptor-triggered immunity by bacterial type-III secretion system effectors. *Current Opinion in Microbiology* 23:14-22.
4. Macho AP (2016) Subversion of plant cellular functions by bacterial type-III effectors: beyond suppression of immunity. *New Phytologist* 210(1):51-57.
5. Cui H, Tsuda K, & Parker JE (2015) Effector-Triggered Immunity: From Pathogen Perception to Robust Defense. *Annual Review of Plant Biology* 66(1):487-511.
6. Chiang Y-H & Coaker G (2015) Effector triggered immunity: NLR immune perception and downstream defense responses. *The Arabidopsis Book*:e0183.
7. Jones JDG & Dangl JL (2006) The plant immune system. *Nature* 444(7117):323-329.
8. Tsuda K & Katagiri F (2010) Comparing signaling mechanisms engaged in pattern-triggered and effector-triggered immunity. *Current Opinion in Plant Biology* 13(4):459-465.
9. Meng X & Zhang S (2013) MAPK cascades in plant disease resistance signaling. *Annual Review of Phytopathology* 51(1):245-266.
10. Tsuda K*, et al.* (2013) Dual regulation of gene expression mediated by extended MAPK activation and salicylic acid contributes to robust innate immunity in *Arabidopsis thaliana*. *PLoS Genetics* 9(12):e1004015.
11. Toruño TY, Stergiopoulos I, & Coaker G (2016) Plant-pathogen effectors: cellular probes interfering with plant defenses in spatial and temporal manners. *Annual Review of Phytopathology* 54(1):419-441.

12. Mansfield J*, et al.* (2012) Top 10 plant pathogenic bacteria in molecular plant pathology. *Molecular Plant Pathology* 13(6):614-629.
13. Jiang G*, et al.* (2017) Bacterial wilt in China: history, current status, and future perspectives. *Frontiers in Plant Science* 8(1549).
14. Turner M*, et al.* (2009) Dissection of bacterial wilt on *Medicago truncatula* revealed two type III secretion system effectors acting on root infection process and disease development. *Plant Physiology* 150(4):1713-1722.
15. Digonnet C*, et al.* (2012) Deciphering the route of *Ralstonia solanacearum* colonization in *Arabidopsis thaliana* roots during a compatible interaction: focus at the plant cell wall. *Planta* 236(5):1419-1431.
16. Peeters N*, et al.* (2013) Repertoire, unified nomenclature and evolution of the Type III effector gene set in the *Ralstonia solanacearum* species complex. *BMC Genomics* 14(1):859.
17. Guéneron M, Timmers ACJ, Boucher C, & Arlat M (2000) Two novel proteins, PopB, which has functional nuclear localization signals, and PopC, which has a large leucine-rich repeat domain, are secreted through the Hrp-secretion apparatus of *Ralstonia solanacearum*. *Molecular Microbiology* 36(2):261-277.
18. Jacobs JM, Babujee L, Meng F, Milling A, & Allen C (2012) The *in planta* transcriptome of *Ralstonia solanacearum* conserved physiological and virulence strategies during bacterial wilt of tomato. *mBio* 3(4):e00114-00112.
19. Puigvert M*, et al.* (2017) Transcriptomes of *Ralstonia solanacearum* during root colonization of *Solanum commersonii*. *Frontiers in Plant Science* 8(370).
20. Deslandes L & Genin S (2014) Opening the *Ralstonia solanacearum* type III effector tool box: insights into host cell subversion mechanisms. *Current Opinion in Plant Biology* 20:110-117.
21. Hayward AC (1991) Biology and epidemiology of bacterial wilt caused by *Pseudomonas solanacearum*. *Annual Review of Phytopathology* 29(1):65-87.
22. Azevedo C*, et al.* (2002) The RAR1 interactor SGT1, an essential component of *R* gene-triggered disease resistance. *Science* 295(5562):2073-2076.
23. Kadota Y, Shirasu K, & Guerois R (2010) NLR sensors meet at the SGT1-HSP90 crossroad. *Trends in Biochemical Sciences* 35(4):199-207.
24. Noël LD*, et al.* (2007) Interaction between SGT1 and cytosolic/nuclear HSC70 chaperones regulates Arabidopsis immune responses. *The Plant Cell* 19(12):4061-4076.
25. Gao Z, Chung E-H, Eitas TK, & Dangl JL (2011) Plant intracellular innate immune receptor Resistance to *Pseudomonas syringae* pv. maculicola 1 (RPM1) is activated at, and functions on, the plasma membrane. *Proceedings of the National Academy of Sciences of the United States of America* 108 (18):7619-7624.
26. Shirasu K (2009) The HSP90-SGT1 chaperone complex for NLR immune sensors. *Annual Review of Plant Biology* 60(1):139-164.
27. Bieri S*, et al.* (2004) RAR1 positively controls steady state levels of barley MLA resistance proteins and enables sufficient MLA6 accumulation for effective resistance. *The Plant Cell* 16(12):3480-3495.

28. Leister RT, *et al.* (2005) Molecular genetic evidence for the role of *SGT1* in the intramolecular complementation of Bs2 protein activity in *Nicotiana benthamiana*. *The Plant Cell* 17(4):1268-1278.
29. Kud J, *et al.* (2013) SGT1 interacts with the Prf resistance protein and is required for Prf accumulation and Prf-mediated defense signaling. *Biochemical and Biophysical Research Communications* 431(3):501-505.
30. Bent A, *et al.* (1994) RPS2 of *Arabidopsis thaliana*: a leucine-rich repeat class of plant disease resistance genes. *Science* 265(5180):1856-1860.
31. Jin H, *et al.* (2002) NPK1, an MEKK1-like mitogen-activated protein kinase kinase kinase, regulates innate immunity and development in plants. *Developmental Cell* 3(2):291-297.
32. Armstrong MR, *et al.* (2005) An ancestral oomycete locus contains late blight avirulence gene *Avr3a*, encoding a protein that is recognized in the host cytoplasm. *Proceedings of the National Academy of Sciences of the United States of America* 102(21):7766-7771.
33. Wei C-F, *et al.* (2007) A *Pseudomonas syringae* pv. *tomato* DC3000 mutant lacking the type III effector HopQ1-1 is able to cause disease in the model plant *Nicotiana benthamiana*. *The Plant Journal* 51(1):32-46.
34. Sang Y, *et al.* (2019) Intra-strain elicitation and suppression of plant immunity by *Ralstonia solanacearum* type-III effectors in *Nicotiana benthamiana*. *bioRxiv*: 780890.
35. Lacomme C & Santa Cruz S (1999) Bax-induced cell death in tobacco is similar to the hypersensitive response. *Proceedings of the National Academy of Sciences* 96(14):7956-7961.
36. Kamoun S, van West P, Vleeshouwers VGAA, de Groot KE, & Govers F (1998) Resistance of *Nicotiana benthamiana* to *Phytophthora infestans* is mediated by the recognition of the elicitor protein INF1. *The Plant Cell* 10(9):1413-1425.
37. Adachi H, *et al.* (2015) WRKY transcription factors phosphorylated by MAPK regulate a plant immune NADPH oxidase in *Nicotiana benthamiana*. *The Plant Cell* 27(9):2645-2663.
38. Popescu SC, *et al.* (2009) MAPK target networks in *Arabidopsis thaliana* revealed using functional protein microarrays. *Genes & Development* 23(1):80-92.
39. Grant M, *et al.* (1995) Structure of the Arabidopsis RPM1 gene enabling dual specificity disease resistance. *Science* 269(5225):843-846.
40. Gassmann W, Hinsch ME, & Staskawicz BJ (1999) The Arabidopsis RPS4 bacterial-resistance gene is a member of the TIR-NBS-LRR family of disease-resistance genes. *The Plant Journal* 20(3):265-277.
41. Hoser R, *et al.* (2013) Nucleocytoplasmic partitioning of tobacco N receptor is modulated by SGT1. *New Phytologist* 200(1):158-171.
42. Kim NH, Kim DS, Chung EH, & Hwang BK (2014) Pepper suppressor of the G2 allele of *skp1* interacts with the receptor-like cytoplasmic kinase1 and type

III effector AvrBsT and promotes the hypersensitive cell death response in a phosphorylation-dependent manner. *Plant Physiology* 165(1):76-91.

43. Redkar A*, et al.* (2015) A secreted effector protein of *Ustilago maydis* guides maize leaf cells to form tumors. *The Plant Cell* 27(4):1332-1351.

44. Cui H*, et al.* (2010) *Pseudomonas syringae* effector protein AvrB perturbs Arabidopsis hormone signaling by activating MAP Kinase 4. *Cell Host & Microbe* 7(2):164-175.

45. Poueymiro M*, et al.* (2009) Two type III secretion system effectors from *Ralstonia solanacearum* GMI1000 determine host-range specificity on tobacco. *Molecular Plant-Microbe Interactions* 22(5):538-550.

46. Macho AP, Guidot A, Barberis P, Beuzón CR, & Genin S (2010) A competitive index assay identifies several *Ralstonia solanacearum* type III effector mutant strains with reduced fitness in host plants. *Molecular plant-microbe interactions* 23(9):1197-1205.

47. Sang Y*, et al.* (2018) The *Ralstonia solanacearum* type-III effector RipAY targets plant redox regulators to suppress immune responses. *Molecular Plant Pathology* 19(1):129-142.

48. Holt BF, Belkhadir Y, & Dangl JL (2005) Antagonistic control of disease resistance protein stability in the plant immune system. *Science* 309(5736):929-932.

49. Azevedo C*, et al.* (2006) Role of SGT1 in resistance protein accumulation in plant immunity. *The EMBO Journal* 25(9):2007-2016.

50. Botër M*, et al.* (2007) Structural and functional analysis of SGT1 reveals that its interaction with HSP90 is required for the accumulation of Rx, an R protein involved in plant immunity. *The Plant Cell* 19(11):3791-3804.

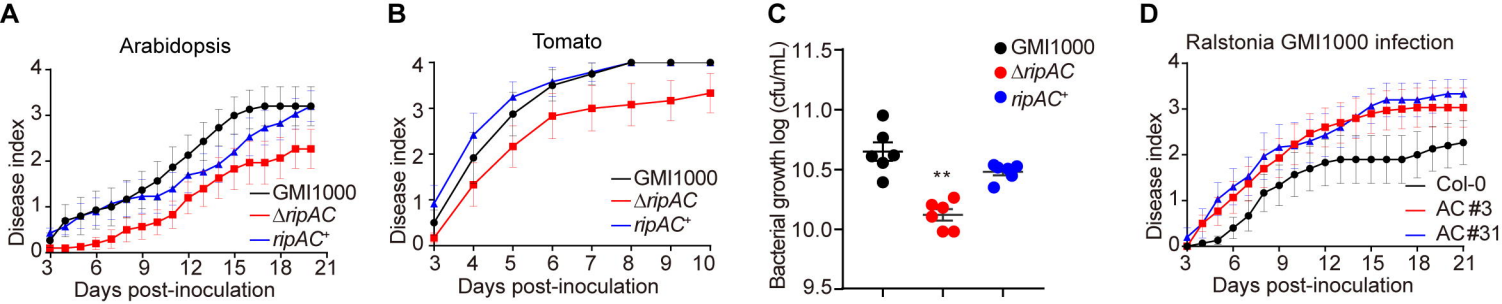
A
Arabidopsis
Disease index
Days post-inoculation
GMI1000
ΔripAC
ripAC+
B
Tomato
Disease index
Days post-inoculation
GMI1000
ΔripAC
ripAC+
C
Bacterial growth log (cfu/mL)
GMI1000
ΔripAC
ripAC+
**
D
Ralstonia GMI1000 infection
Disease index
Days post-inoculation
Col-0
AC #3
AC #31

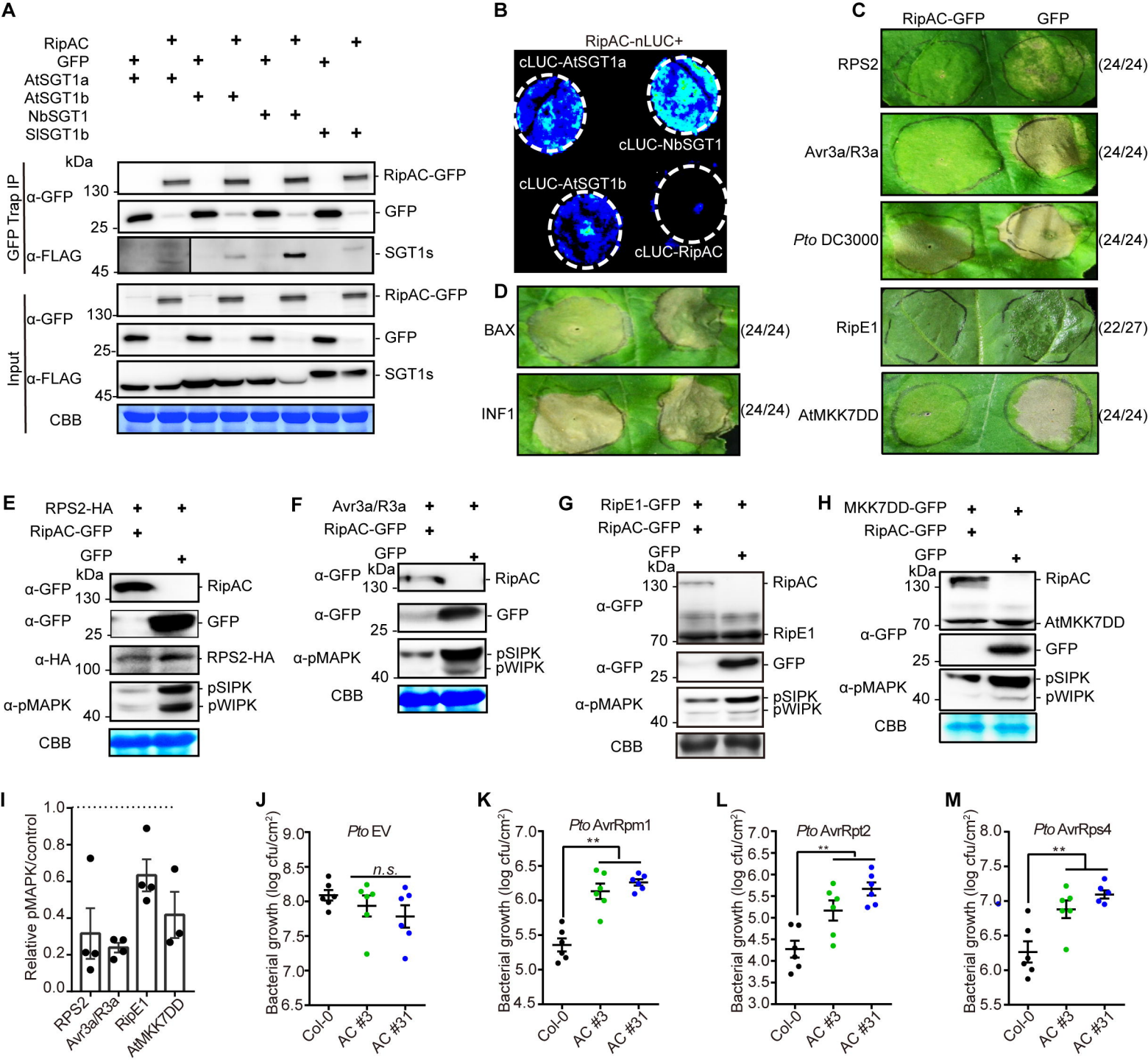
A
RipAC
GFP
AtSGT1a
AtSGT1b
NbSGT1
SlSGT1b
kDa
GFP Trap IP
α-GFP
α-FLAG
Input
CBB
RipAC-GFP
GFP
SGT1s
B
RipAC-nLUC+
cLUC-AtSGT1a
cLUC-NbSGT1
cLUC-AtSGT1b
cLUC-RipAC
C
RipAC-GFP
GFP
RPS2
Avr3a/R3a
Pto DC3000
RipE1
AtMKK7DD
(24/24)
(22/27)
D
BAX
INF1
E
RPS2-HA
α-HA
α-pMAPK
pSIPK
pWIPK
F
Avr3a/R3a
G
RipE1-GFP
H
MKK7DD-GFP
I
Relative pMAPK/control
RPS2
Avr3a/R3a
RipE1
AtMKK7DD
J
Pto EV
n.s.
Bacterial growth (log cfu/cm2)
Col-0
AC #3
AC #31
K
Pto AvrRpm1
**
L
Pto AvrRpt2
M
Pto AvrRps4

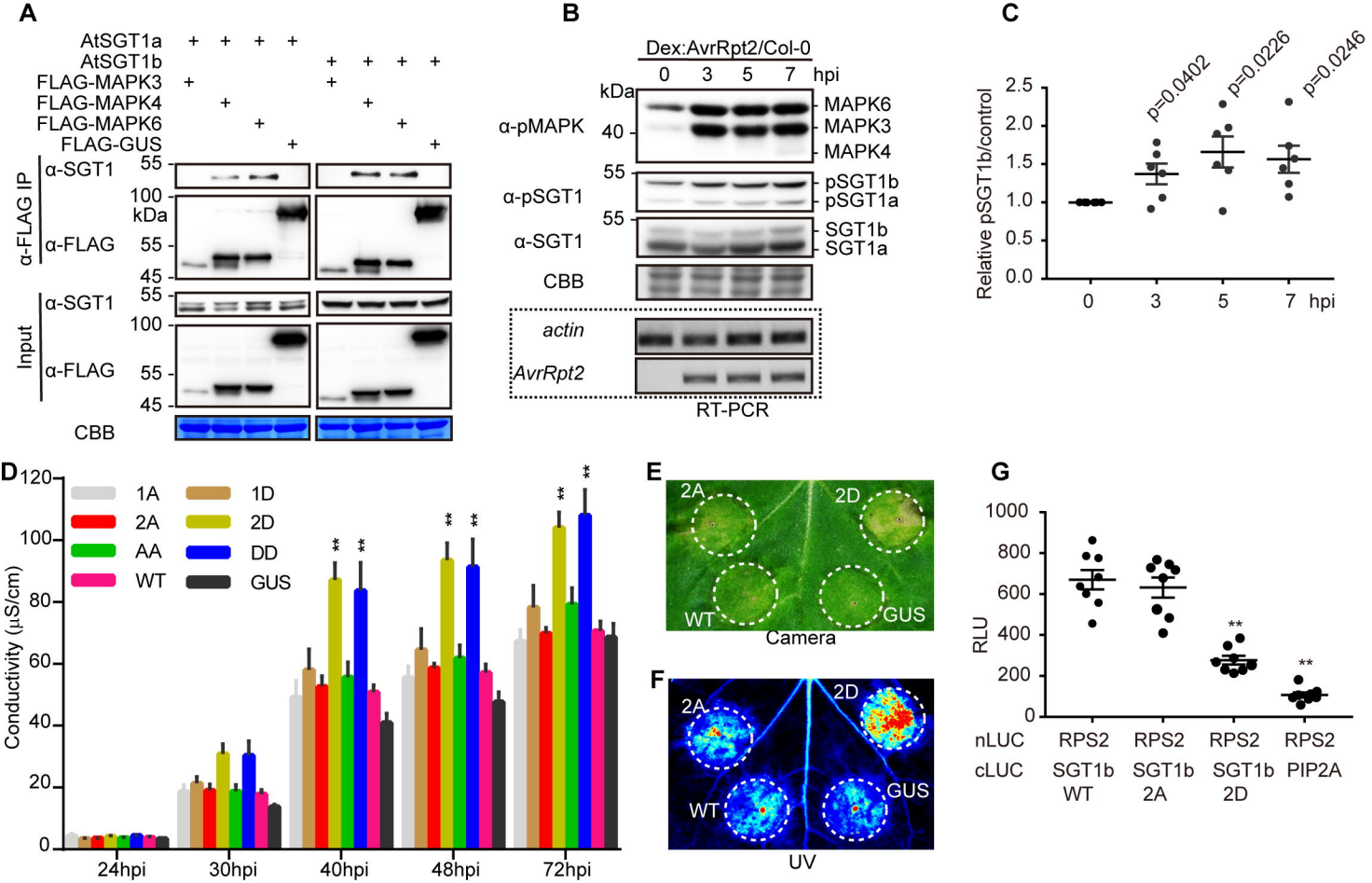
A
AtSGT1a
AtSGT1b
FLAG-MAPK3
FLAG-MAPK4
FLAG-MAPK6
FLAG-GUS
α-FLAG IP
α-SGT1
α-FLAG
Input
CBB
kDa
B
Dex:AvrRpt2/Col-0
0 3 5 7 hpi
α-pMAPK
MAPK6
MAPK3
MAPK4
α-pSGT1
pSGT1b
pSGT1a
α-SGT1
SGT1b
SGT1a
CBB
actin
AvrRpt2
RT-PCR
C
Relative pSGT1b/control
p=0.0402
p=0.0226
p=0.0246
0 3 5 7 hpi
D
1A
2A
AA
WT
1D
2D
DD
GUS
Conductivity (μS/cm)
24hpi
30hpi
40hpi
48hpi
72hpi
E
2A
2D
WT
GUS
Camera
F
UV
G
RLU
nLUC
cLUC
RPS2
SGT1b WT
SGT1b 2A
SGT1b 2D
PIP2A

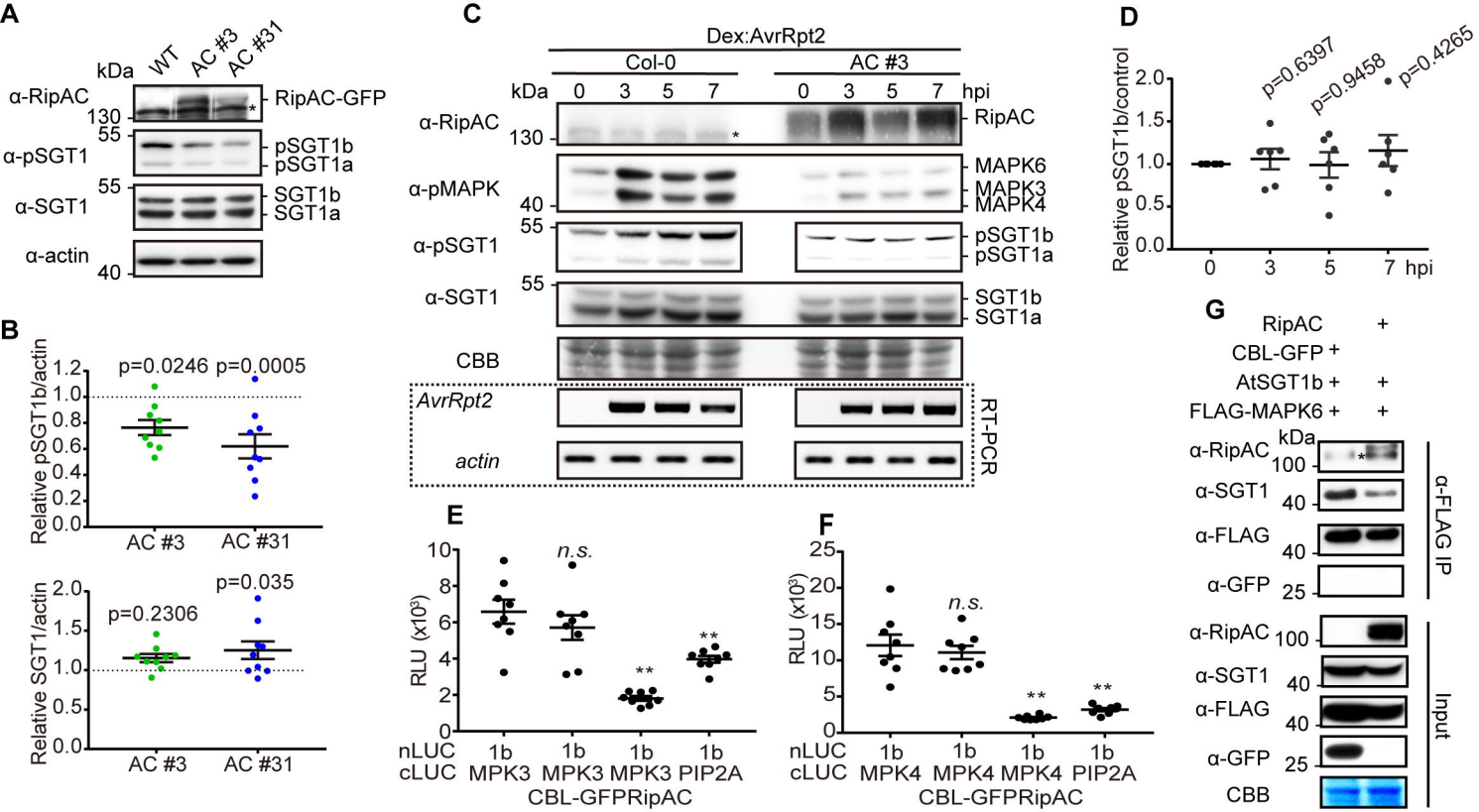
A
kDa
WT
AC #3
AC #31
α-RipAC
RipAC-GFP
130
55
α-pSGT1
pSGT1b
pSGT1a
55
α-SGT1
SGT1b
SGT1a
α-actin
40
B
p=0.0246
p=0.0005
Relative pSGT1b/actin
AC #3
AC #31
p=0.2306
p=0.035
Relative SGT1/actin
C
Dex:AvrRpt2
Col-0
AC #3
kDa
0 3 5 7
0 3 5 7 hpi
α-RipAC
RipAC
130
α-pMAPK
MAPK6
MAPK3
MAPK4
40
55
α-pSGT1
pSGT1b
pSGT1a
55
α-SGT1
SGT1b
SGT1a
CBB
AvrRpt2
actin
RT-PCR
D
p=0.6397
p=0.9458
p=0.4265
Relative pSGT1b/control
0 3 5 7 hpi
E
n.s.
RLU (x10³)
nLUC 1b 1b 1b 1b
cLUC MPK3 MPK3 MPK3 PIP2A
CBL-GFPRipAC
F
n.s.
RLU (x10³)
nLUC 1b 1b 1b 1b
cLUC MPK4 MPK4 MPK4 PIP2A
CBL-GFPRipAC
G
RipAC +
CBL-GFP +
AtSGT1b + +
FLAG-MAPK6 + +
kDa
α-RipAC
100
α-SGT1
40
α-FLAG
40
α-GFP
25
α-FLAG IP
α-RipAC
100
α-SGT1
40
α-FLAG
40
α-GFP
25
CBB
Input